PHYSICAL REVIEW A VOLUME 17, NUMBER 1 JANUARY 1978

Numerical experiment on two-dimensional electron liquids. Thermodynamic properties and onset of short-range order

Hiroo Totsuji

Department of Physics, University of Tokyo, Bunkyo-ku, Tokyo 113
and Department of Electronics, Okayama University, Tsushimanaka, Okayama 700, Japan †

(Received 21 June 1977)

Thermodynamic properties of two-dimensional electron liquids are determined by numerical experiments over the domain of the plasma parameter $\epsilon = 2\pi ne^4/T^2$, $0.05 \leq \epsilon \leq 5 \times 10^3$, where n, e, and T denote the number density, the unit charge, and the temperature in energy units, respectively. The correlation energy thus obtained is consistent with both the result of the plasma-parameter expansion calculation and that of earlier numerical experiments in the high-density domain. The pair correlation function $g(r)$ agrees with the analytical result when ϵ is small. Short-range order appears at the critical plasma parameter ϵ_{sr} in the range $10 < \epsilon_{sr} < 15$. It is pointed out that the two-dimensional screening function $h(r) = \ln[g(r)+1] + e^2/Tr$ is approximately a linear function of the radius r in the short-range domain, as in the case of three dimensions.

I. INTRODUCTION

On the surfaces of dielectric substances such as liquid He there are two-dimensional systems of electrons interacting via the Coulomb potential, with the effective charge nearly equal to a unit charge[1] in the uniform background provided by a positively charged metallic plate. Since the quantum effects can be neglected in most experimental conditions,[1,2] these systems in thermal equilibrium are characterized by the dimensionless plasma parameter defined by $\epsilon = 2\pi ne^4/T^2$ or the parameter $\Gamma = (\epsilon/2)^{1/2}$, where n, e, and T are the number density, the (effective) electronic charge, and the temperature in energy units, respectively.

A characteristic feature of Coulombic systems is an interplay between their collective and individual-particle aspects. In two-dimensional electron liquids, the role of the individual-particle aspect becomes more important than in three-dimensional ones[2]; for example, when the plasma parameter is small, the contribution of the short-range correlations to the correlation energy is comparable with that of the long-range correlations, and the collective aspect can be neglected in collisional processes.

In theoretical investigations of three-dimensional electron liquids, the numerical experiments by Brush, Sahlin, and Teller[3] and by Hansen[4] have been quite useful. For two-dimensional electron liquids, we have no such experimental information except that related to the Wigner lattice formation in the very-high-density domain $\epsilon \simeq 2 \times 10^4$ due to Hockney and Brown.[5] The purpose of our numerical experiments is to investigate thermodynamic properties of two-dimensional electron liquids for the range of the plasma parameter $0.05 \leq \epsilon \leq 5 \times 10^3$ which includes the low-, intermediate-, and high-density domains. In the low-density domain, we confirm the consistency of our results with analytical calculations[2,6] based on the plasma-parameter expansion. In the domain of intermediate density, the pair correlation function changes from a monotonous to an oscillating function of radius. The critical plasma parameter for this onset of the short-range order is determined to be in a small range. In the high-density domain, we find that the pair correlation function can be represented in terms of a linear screening function. The consistency with the result due to Hockney and Brown[5] in the very-high-density domain is also confirmed. We expect that these results may be useful for theoretical analyses of electron liquids in two dimensions and also for elucidating the properties of three-dimensional ones through the aforementioned difference due to dimensionality.

II. METHOD

We simulate the equilibrium distribution by the Monte Carlo method[7] which has been used by Brush *et al.*[3] and by Hansen.[4] We produce the chain of configurations of particles by randomly displacing them so that the chain may realize the canonical distribution.

The essential part of the numerical computation is that of the interaction energy in each step of the chain. Due to the long-range nature of the Coulomb interaction, some device is necessary to calculate the interaction energy of an infinitely extended system. It has been shown[3,4] that the three-dimensional infinite system can be simulated by the periodic system with rather small number of particles in the unit cell. We thus

adopt the periodic system, denoting the area of the unit cell and the number of particles in it by S_0 and N_0, and ascertain that the results are independent of the use of the periodic system by changing the symmetry of the periodicity and the number of particles in the unit cell.

In the uniform background, the Coulomb interaction is given by

$$\frac{e^2}{S}\sum_{\vec{k}}{}' \frac{2\pi}{k}\exp(i\vec{k}\cdot\vec{r}), \tag{2.1}$$

where S is the area of the system and the prime indicates that the term with $\vec{k}=0$ is omitted. The interaction energy $v(\vec{r}_{ij})$ between the particle i (at $\vec{r}_i$) and particle j (at $\vec{r}_j$) and its periodic images (at $\vec{r}_j+\vec{p}$) is given by

$$v(\vec{r}_{ij}) = \sum_{\vec{p}}\frac{e^2}{S}\sum_{\vec{k}}{}'\frac{2\pi}{k}\exp[i\vec{k}\cdot(\vec{r}_{ij}-\vec{p})]$$

$$= \frac{e^2}{S_0}\sum_{\vec{g}}{}'\frac{2\pi}{g}\exp(i\vec{g}\cdot\vec{r}_{ij}), \tag{2.2}$$

where $\vec{r}_{ij}=\vec{r}_i-\vec{r}_j$, and $\vec{p}$ and $\vec{g}$ denote the vectors of the periodic lattice and the reciprocal lattice, respectively. Rewriting $1/g$ as

$$\frac{1}{g} = \frac{2}{\sqrt{\pi}}\left(\int_0^R + \int_R^\infty\right)dt\exp(-g^2t^2), \tag{2.3}$$

we divide $v(\vec{r})$ into the short-range part $v_s(\vec{r})$ and the long-range part $v_l(\vec{r})$ using the well-known Ewald method. We have finally

$$v(\vec{r}) = v_l(\vec{r}) + v_s(\vec{r}) - (4\sqrt{\pi}/S_0)Re^2, \tag{2.4}$$

where

$$v_l(\vec{r}) = \frac{e^2}{S_0}\sum_{\vec{g}}{}'\frac{2\pi}{g}\operatorname{erfc}(gR)\exp(i\vec{g}\cdot\vec{r}), \tag{2.5}$$

$$v_s(\vec{r}) = \sum_{\vec{p}}\frac{e^2}{|\vec{r}-\vec{p}|}\operatorname{erfc}\left(\frac{|\vec{r}-\vec{p}|}{2R}\right), \tag{2.6}$$

and

$$\operatorname{erfc}(x) = \frac{2}{\sqrt{\pi}}\int_x^\infty dt\,\exp(-t^2). \tag{2.7}$$

The interaction energy between a particle and its own periodic images is the Madelung energy U_M of the lattice $\vec{p}$ which is given by

$$U_M = \lim_{r\to 0}\left(\frac{1}{S_0}\sum_{\vec{g}}{}'\frac{2\pi e^2}{g}\exp(i\vec{g}\cdot\vec{r}) - \frac{e^2}{r}\right). \tag{2.8}$$

The interaction energy U per unit cell,

$$U = \frac{1}{2}\sum_{i\neq j}^{N_0} v(\vec{r}_{ij}) + N_0U_0,$$

where $U_0 = U_M/2$, is thus calculated as

$$U = \frac{1}{2}\sum_{i\neq j}^{N_0} v_s(\vec{r}_{ij}) + \frac{1}{2}\sum_{\vec{g}}{}'\frac{2\pi e^2}{g}\operatorname{erfc}(gR)(\rho_{\vec{g}}\rho_{-\vec{g}} - N_0)$$
$$+ N_0U_0 - N_0(N_0-1)(2\sqrt{\pi}/S_0)Re^2, \tag{2.9}$$

where

$$\rho_{\vec{g}} = \sum_{i=1}^{N_0}\exp(-i\vec{g}\cdot\vec{r}_i).$$

In Eq. (2.9), both the first and the second terms converge rapidly. We use Eq. (2.9) optimizing the computational time with respect to the parameter R. The Madelung energies for the hexagonal and square lattices are calculated as

$$U_0(\text{hexagonal}) = -2.106\,711\,318\,07e^2/a, \tag{2.10}$$

and

$$U_0(\text{square}) = -1.950\,132\,460\,00e^2/a, \tag{2.11}$$

where a is the lattice constant.

III. RESULTS

In the domain $\epsilon \leq 5\times 10^3$, several thousands of steps are sufficient to eliminate the effect of the initial configuration in the Monte Carlo chain. We discard more than 8×10^3 steps in the initial part of the chain. As the initial distribution, we take a random distribution or a complete lattice.

In Table I, we show the values of the correlation energy density E_c normalized by the kinetic-energy density nT for the hexagonal and square symmetries and for $N_0=36$ and $N_0=81$ at the same value of the plasma parameter $\epsilon = 1\times 10^3$. We see that the resultant values do not depend on the symmetry and 36 is sufficient as the number of independent particles. Having thus confirmed that the experimental results do not depend on the boundary condition and the value of N_0, we adopt the hexagonal symmetry and $N_0=81$.

In the two-dimensional Coulomb system, the Helmholtz free energy F, the internal energy E, and the specific heat at constant volume C_V are calculated from the ratio of the correlation-energy density to the kinetic-energy density E_c/nT as

$$F = F_0 + \frac{NT}{2}\int_0^\epsilon \frac{d\epsilon}{\epsilon}\frac{E_c}{nT}, \tag{3.1}$$

TABLE I. The correlation energy normalized by the kinetic energy E_c/nT for different boundary conditions and for different numbers of independent particles.

	Hexagonal	Square
$N_0=81$	-23.83 ± 0.10	-23.82 ± 0.10
$N_0=36$	-23.80 ± 0.14	

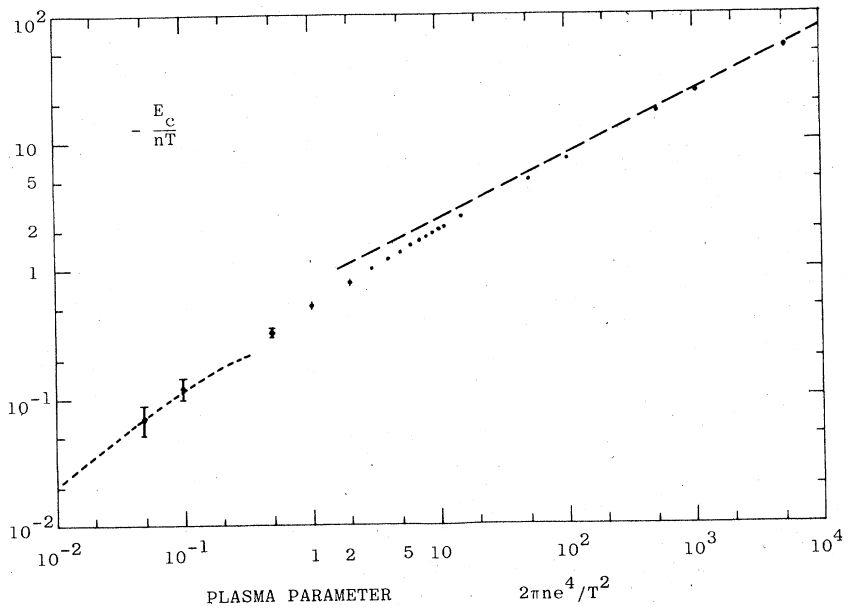

FIG. 1. Correlation energy normalized by the kinetic energy vs the plasma parameter. Filled circles are experimental values. The dotted and broken lines describe the result of the plasma-parameter-expansion analysis and the Madelung values for two-dimensional Coulomb lattices.

$$E = F - T\left(\frac{\partial F}{\partial T}\right)_V = NT\left(1 + \frac{E_c}{nT}\right), \tag{3.2}$$

and

$$C_V = \left(\frac{\partial E}{\partial T}\right)_V = N\left(1 + \frac{E_c}{nT} - 2\epsilon\frac{\partial}{\partial\epsilon}\frac{E_c}{nT}\right). \tag{3.3}$$

Here F_0 is the free energy of the ideal gas and N is the total number of electrons.

Values of E_c/nT are shown in Fig. 1 and Table II for the range of the plasma parameter $0.05 \leq \epsilon \leq 5\times10^3$. In Fig. 1, we also plot (dotted line) the values based on the plasma parameter expansion[2,6]

$$E_c/nT = \tfrac{1}{2}\epsilon\ln 2\epsilon + \epsilon(\gamma - \tfrac{1}{2}) - \tfrac{1}{2}\epsilon^2\ln^2\tfrac{1}{2}\epsilon + (1-2\gamma)\epsilon^2\ln\epsilon + \cdots \tag{3.4}$$

(where $\gamma = 0.5772\cdots$), and (broken line) the Madelung values for the lattice ($U_0 = U_0'e^2/a$)

$$E_c/nT = 3^{1/4}(4\pi)^{-1/2}U_0'\epsilon^{1/2} = -0.7821\epsilon^{1/2} = -1.1061\Gamma(\text{hexagonal}) \tag{3.5}$$

or

$$E_c/nT = (2\pi)^{-1/2}U_0'\epsilon^{1/2} = -0.7780\epsilon^{1/2} = -1.1002\Gamma(\text{square}). \tag{3.6}$$

When the plasma parameter is small, our results are consistent with the result of the plasma parameter expansion. For large values of the plasma parameter, the correlation energy is nearly equal to the Madelung values and our results are consistent with those of Hockney and

TABLE II. The correlation energy normalized by the kinetic energy E_c/nT and the number of effective steps in the Monte Carlo chain for various values of the plasma parameter $\epsilon = 2\pi ne^4/T^2$.

ϵ	E_c/nT	Steps	ϵ	E_c/nT	Steps
5×10^{-2}	-0.068 ± 0.019	1.56×10^5	8	-1.78 ± 0.06	1.24×10^5
1×10^{-1}	-0.118 ± 0.022	1.34×10^5	9	-1.90 ± 0.06	1.16×10^5
5×10^{-1}	-0.32 ± 0.03	3.2×10^4	10	-2.03 ± 0.06	1.06×10^5
1	-0.52 ± 0.03	5.4×10^4	11	-2.12 ± 0.07	7.2×10^4
2	-0.78 ± 0.04	5.6×10^4	15	-2.53 ± 0.06	5.2×10^4
3	-1.00 ± 0.04	3.2×10^4	5×10	-4.93 ± 0.07	3.2×10^4
4	-1.19 ± 0.04	3.2×10^4	1×10^2	-7.14 ± 0.07	2.2×10^4
5	-1.34 ± 0.05	5.6×10^4	5×10^2	-16.63 ± 0.09	2.4×10^4
6	-1.51 ± 0.03	7.2×10^4	1×10^3	-23.83 ± 0.10	2.2×10^4
7	-1.65 ± 0.05	1.24×10^5	5×10^3	-54.18 ± 0.10	1.8×10^4

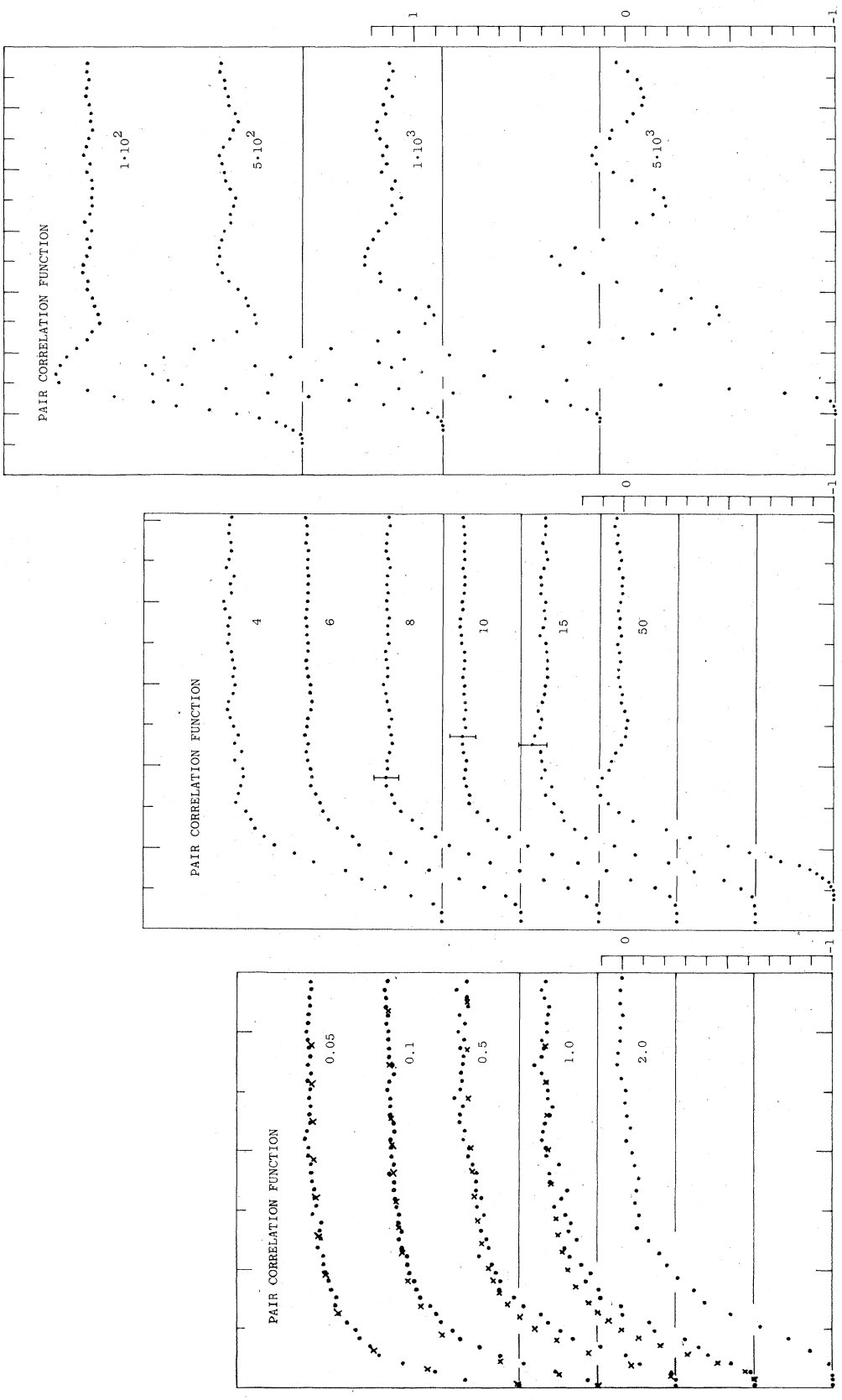

FIG. 2. Pair correlation function as a function of the reduced distance $(\pi n)^{1/2}r$. Figures attached to curves denote the values of the plasma parameter. The crosses represent the values given by Eq. (3.13).

TABLE III. Pair correlation function $g(r)$ for various values of the plasma parameter $\epsilon = 2\pi ne^4/T^2$. Values of $g(r)+1$ are tabulated. $r_1 = 3.428 \times 10^{-2}(\pi n)^{-1/2}$.

	ϵ					ϵ			
r/r_1	0.05	0.1	0.5	1.0	r/r_1	0.05	0.1	0.5	1.0
2	0.25	0.06			42	0.98	0.93	0.91	0.89
4	0.40	0.21	0.02	0.02	44	0.96	0.95	0.94	0.95
6	0.55	0.36	0.17	0.11	46	0.97	0.96	0.92	0.91
8	0.67	0.46	0.24	0.22	48	0.97	0.97	0.95	0.88
10	0.71	0.58	0.36	0.26	50	0.98	0.96	0.94	0.97
12	0.76	0.66	0.49	0.32	52	0.99	0.98	0.94	0.97
14	0.77	0.68	0.55	0.47	54	0.99	0.97	0.96	0.92
16	0.82	0.74	0.60	0.50	56	1.00	0.98	0.98	0.98
18	0.86	0.77	0.63	0.62	58	1.00	0.98	0.98	0.99
20	0.87	0.79	0.72	0.63	60	1.01	0.99	1.01	1.00
22	0.86	0.84	0.77	0.72	62	1.01	0.96	1.00	1.00
24	0.89	0.86	0.83	0.73	64	0.99	0.98	1.02	0.99
26	0.90	0.86	0.83	0.80	66	0.99	0.99	1.02	0.97
28	0.92	0.88	0.85	0.78	68	0.99	0.98	1.00	0.95
30	0.93	0.90	0.87	0.82	70	1.00	0.98	1.05	0.98
32	0.93	0.91	0.93	0.87	72	0.99	0.99	1.02	0.98
34	0.96	0.93	0.88	0.89	74	1.00	0.98	1.01	0.98
36	0.94	0.94	0.89	0.84	76	0.99	0.97	1.02	1.01
38	0.94	0.93	0.92	0.87	78	1.00	0.97	1.01	1.04
40	0.94	0.94	0.94	0.87	80	0.99	0.98	1.01	1.01

Brown.[5,8]

Recently, DeWitt[9] has proposed an interpolation formula for the correlation energy of the three-dimensional classical electron liquids in the form

$$E_c/nT = a\Gamma + b\Gamma^s + c\,, \tag{3.7}$$

where the three-dimensional parameter Γ is defined by $\Gamma = (4\pi n/3)^{1/3}e^2/T$ and $s \simeq 1/4$. The first term on the right-hand side is nearly equal to the Madelung value and the second and the third terms represent the excess thermal energy.

In the two-dimensional case, we find that the values of the correlation energy for $1 \leq \epsilon \leq 5\times 10^3$ can be represented by the formula of the same

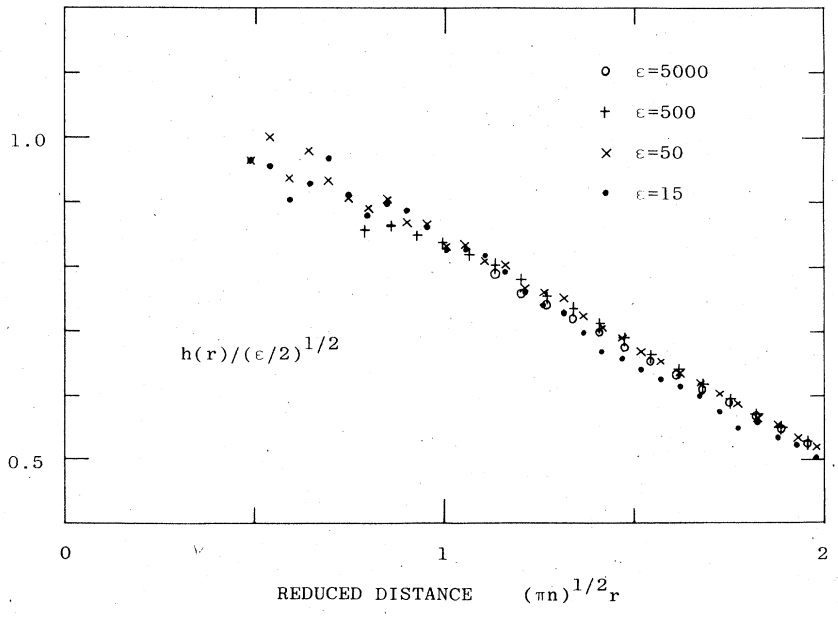

FIG. 3. The two-dimensional screening function $h(r) = \ln[g(r)+1] + (e^2/Tr)$ as a function of the reduced distance $(\pi n)^{1/2}r$. The ordinate expresses the values of $h(r)/(\epsilon/2)^{1/2}$.

TABLE IV. The same as Table III. $r_2 = 5.143\times10^{-2}(\pi n)^{-1/2}$.

r/r_2	ϵ 2	4	6	8	10	15	50
2	0.002						
4	0.02	0.002			0.001		
6	0.11	0.04	0.03	0.01	0.008	0.006	
8	0.21	0.15	0.07	0.06	0.03	0.02	
8.5							0.003
9.5							0.004
10	0.35	0.27	0.18	0.15	0.10	0.07	
10.5							0.014
11.5							0.023
12	0.49	0.38	0.29	0.26	0.22	0.15	
12.5							0.056
13.5							0.080
14	0.61	0.46	0.43	0.38	0.33	0.29	
14.5							0.113
15.5							0.161
16	0.66	0.61	0.55	0.52	0.47	0.41	
16.5							0.252
17.5							0.299
18	0.74	0.70	0.62	0.62	0.59	0.57	
18.5							0.399
20	0.79	0.80	0.77	0.71	0.70	0.67	0.503
22	0.83	0.84	0.80	0.78	0.80	0.81	0.680
24	0.88	0.89	0.87	0.84	0.86	0.86	0.793
26	0.93	0.91	0.91	0.89	0.89	0.91	0.950
28	0.92	0.93	0.94	0.94	0.94	0.92	1.019
30	0.95	0.98	0.95	0.97	0.98	0.96	1.070
32	0.94	0.97	0.97	0.98	0.98	1.00	1.107
34	0.93	0.95	0.99	1.01	1.00	0.97	1.118
36	0.95	0.95	0.99	1.01	1.01	1.02	1.099
38	0.96	0.95	0.99	1.00	1.00	1.00	1.067
40	0.99	0.98	1.01	1.01	1.00	1.02	1.051
42	0.97	0.96	1.01	1.00	1.01	1.02	1.033
44	0.98	0.98	1.01	0.98	1.02	1.06	1.005
46	0.99	0.97	1.02	0.99	1.01	1.05	0.987
48	0.99	0.99	1.01	1.00	1.00	1.03	0.982
50	1.01	1.01	1.01	0.99	1.01	1.02	0.979
52	1.03	1.02	0.99	1.00	1.00	1.04	0.989
54	1.03	1.02	0.99	1.01	1.00	1.02	1.004
56	1.02	0.99	1.00	1.02	1.01	1.01	1.001
58	1.02	0.99	0.99	1.03	1.00	1.00	1.013
60	1.00	0.99	1.00	1.01	1.01	0.99	1.020
62	1.02	0.99	1.01	1.01	1.01	1.00	1.021
64	1.01	1.00	1.01	1.02	1.01	0.99	1.009
66	1.01	1.01	1.01	1.02	1.01	1.00	1.013
68	1.01	1.02	1.01	1.00	1.02	1.00	1.023
70	1.02	1.02	1.01	1.01	1.02	1.03	1.008
72	1.01	1.02	1.01	1.01	1.03	1.02	1.016
74	1.00	1.01	1.02	1.00	1.03	1.01	1.011
76	1.01	1.03	1.01	1.01	1.01	1.01	1.020
78	1.02	1.04	1.01	1.01	1.02	1.00	1.011
80	1.02	1.00	1.01	1.01	1.01	1.03	0.999

type as Eq. (3.7),

$$E_c/nT = -0.79\epsilon^{1/2} + 0.65\epsilon^{1/8} - 0.38$$
$$= -1.12\Gamma + 0.71\Gamma^{1/4} - 0.38\,, \qquad (3.8)$$

with the error less than 1%. The exponent of the second term, however, cannot be determined uniquely because of the smallness of the range of values of ϵ^s with $s \simeq \frac{1}{8}$. For example, the formula

$$E_c/nT = -0.80\epsilon^{1/2} + 0.52\epsilon^{1/6} - 0.24$$
$$= -1.13\Gamma + 0.58\Gamma^{1/3} - 0.24 \qquad (3.9)$$

or

$$E_c/nT = -0.79\epsilon^{1/2} + 0.85\epsilon^{1/10} - 0.58$$
$$= -1.12\Gamma + 0.91\Gamma^{1/5} - 0.58 \qquad (3.10)$$

can also reproduce the results for $1 \leqslant \epsilon \leqslant 5\times10^3$ with the error nearly the same as Eq. (3.8). In the domain $0.05 \leqslant \epsilon \leqslant 5\times10^3$, our results are represented by the formula

$$E_c/nT = -0.78\epsilon^{1/2} + 0.53\epsilon^{1/8} - 0.26$$
$$= -1.10\Gamma + 0.58\Gamma^{1/4} - 0.26 \qquad (3.11)$$

with the error less than 8% (less than 2% for $0.5 \leqslant \epsilon \leqslant 5\times10^3$), or by the formula

$$E_c/nT = -\epsilon^{1/2}[0.76 - 1/(2.2\epsilon^{1/2} + 1.8)]$$
$$= -\Gamma[1.07 - 1/(2.2\Gamma + 1.3)], \qquad (3.12)$$

with the error less than 6% (less than 2% for $0.5 \leqslant \epsilon \leqslant 5\times10^3$).

The values of the pair correlation function $g(r)$ are shown in Fig. 2 and in Tables III–V. When the plasma parameter is small, the pair correlation function is calculated as[2]

$$g(r) = \exp[-u(r)/T] - 1\,, \qquad (3.13)$$

where

$$u(r) = \frac{e^2}{r}\int_0^\infty dx\, J_0(x)\frac{x}{x + k_D r}\,,$$

$J_0(x)$ is the Bessel function, and $k_D = 2\pi n e^2/T$. The values given by (3.13) are plotted by crosses in Fig. 2 for $\epsilon \leqslant 1.0$. For $\epsilon = 0.05$, experimental results agree with Eq. (3.13). As the plasma parameter increases, the correlation function deviates from Eq. (3.13) in the short-range domain $r \simeq e^2/T$. With further increase of the plasma parameter, the oscillation around the zero level appears. Noting the errors which associate the values of $g(r)$ as shown for $\epsilon = 8$, 10, and 15 in Fig. 2, we observe that the critical value for the onset of the short-range order is in the range

$$10 < \epsilon_{sr} < 15 \quad \text{or} \quad 2.2 < \Gamma_{sr} < 2.7\,. \qquad (3.14)$$

On the other hand, the isothermal compressibility χ_T defined by

$$\chi_T^{-1} = n(\partial P/\partial n)_T\,, \qquad (3.15)$$

where $P = \frac{1}{2}E_c + nT$ is the pressure, diverges at $\epsilon = \epsilon_c = 4.4 \pm 0.1$ or $\Gamma = \Gamma_c = 1.48 \pm 0.02$ according to the interpolation formulas (3.8)–(3.12). Thus, as

TABLE V. The same as Table III. $r_3 = 6.857 \times 10^{-2}(\pi n)^{-1/2}$.

	ϵ					ϵ			
r/r_3	100	500	1000	5000	r/r_3	100	500	1000	5000
7.5	0.001				42	0.995	0.927	0.869	0.686
8.5	0.001				44	1.018	0.966	0.945	0.827
9.5	0.008				46	1.015	1.007	1.037	1.040
10.5	0.044				48	1.041	1.040	1.040	1.199
11.5	0.081	0.001			50	1.037	1.062	1.111	1.313
12.5	0.123	0.008			52	1.019	1.052	1.111	1.351
13.5	0.203	0.027	0.003		54	1.008	1.054	1.096	1.242
14.5	0.311	0.071	0.016		56	1.021	1.041	1.070	1.106
15.5	0.443	0.141	0.060		58	0.997	1.027	1.046	1.024
16.5	0.599	0.280	0.139	0.010	60	1.028	0.996	1.009	0.948
17.5	0.707	0.444	0.250	0.024	62	1.007	0.999	0.964	0.873
18.5	0.891	0.632	0.426	0.090	64	0.996	0.985	0.982	0.801
19.5		0.824	0.696	0.244	66	0.998	0.972	0.939	0.824
20	1.015				68	0.994	1.000	0.984	0.865
20.5		1.022	0.948	0.505	70	0.998	1.022	0.968	0.972
21.5		1.232	1.154	0.834	72	1.019	1.028	1.031	1.058
22	1.152				74	1.007	1.039	1.007	1.139
22.5		1.300	1.313	1.279	76	1.040	1.052	1.028	1.156
23.5				1.668	78	1.024	1.034	1.006	1.143
24	1.164	1.372	1.549		80	1.013	1.000	1.038	1.075
24.5				1.962	82	0.996	0.989	1.058	1.067
26	1.144	1.406	1.627	2.135	84	1.007	0.962	1.051	0.995
28	1.115	1.317	1.463	1.935	86	1.001	0.979	1.012	0.969
30	1.065	1.175	1.268	1.500	88	1.013	1.008	1.020	0.928
32	1.019	1.082	1.051	1.091	90	1.027	1.007	0.977	0.917
34	0.997	0.970	0.950	0.820	92	1.026	1.024	1.010	0.934
36	0.958	0.879	0.824	0.606	94	1.014	1.028	0.994	0.949
38	0.970	0.885	0.783	0.559	96	1.027	1.048	0.979	0.993
40	0.986	0.915	0.810	0.567	98	1.021	1.043	0.993	1.048

in the case of three dimensions,[11] the onset of the short-range order occurs near the critical density where the isothermal compressibility diverges.

In the three-dimensional electron liquids, the screening function $h(r)$ defined by

$$g(r) = \exp[-(e^2/Tr) + h(r)] - 1 \tag{3.16}$$

is accurately represented by a linear function of r in the short-range domain.[12,13] The values of the two-dimensional screening function are shown in Fig. 3 for $15 \leq \epsilon \leq 5 \times 10^3$. It is clear that the two-dimensional screening function can also be represented by a linear function for $50 \leq \epsilon \leq 5 \times 10^3$. We have finally

$$h(r) = \Gamma[1.18 - 0.33(\pi n)^{1/2} r] \tag{3.17}$$

as an interpolation formula for $50 \leq \epsilon \leq 5 \times 10^3$.

ACKNOWLEDGMENTS

The author wishes to thank Professor S. Ichimaru for encouragement and discussions. Thanks are also due to C. Totsuji for her help in programming. Numerical computations are made at the Computer Center of the University of Tokyo and at the Computer Center of the Okayama University.

†Present address.

[1]For example, M. W. Cole, Rev. Mod. Phys. 46, 451 (1974).

[2]H. Totsuji, J. Phys. Soc. Jpn. 39, 253 (1975); 40, 857 (1976).

[3]S. G. Brush, H. L. Sahlin, and E. Teller, J. Chem. Phys. 45, 2102 (1966).

[4]J. P. Hansen, Phys. Rev. A 8, 3096 (1973).

[5]R. W. Hockney and T. R. Brown, J. Phys. C 8, 1813 (1975).

[6]J. Chalupa, Phys. Rev. B 12, 4 (1975). The second term of this result should be corrected as in Ref. 2.

[7]N. Metropolis, A. W. Rosenbluth, A. H. Teller, and E. Teller, J. Chem. Phys. 21, 1087 (1953).

[8]When the temperature tends to zero, the internal energy per electron $U = E/N$ approaches the value given by

Eqs. (3.2) and (3.5) or $U(T=0)/k_B = -327.62$ K for $n = 10^{10}$ cm^{-2}. It seems that the ordinate of Fig. 1 in Ref. 5 has to be slided so that U/k_B tends to this value. Our values of $[U - U(T=0)]/k_B$ and C_V are consistent with their results within experimental errors.

[9]H. E. DeWitt, Phys. Rev. A 14, 1290 (1976).

[10]The formula $E_c/nT = -0.78\epsilon^{1/2} + 0.18\ln\epsilon^{1/2} + 0.25 = -1.10\Gamma + 0.18\ln\Gamma + 0.31$ also reproduces the results with about the same accuracy. The author is indebted to Professor H. E. DeWitt for this fitting.

[11]The nature of thermodynamic instability at $\epsilon = \epsilon_c$ has been clarified in H. Totsuji and S. Ichimaru, Prog. Theor. Phys. (Kyoto) 52, 42 (1974).

[12]H. E. DeWitt, H. C. Graboske, and M. S. Cooper, Atrophys. J. 181, 439 (1973).

[13]N. Itoh, H. Totsuji, and S. Ichimaru, Atrophys. J. (to be published).